

THE LONGITUDINAL AND TRANSVERSE RESPONSES IN THE INCLUSIVE ELECTRON SCATTERING

R. Cenni, F. Conte and P. Saracco

Istituto Nazionale di Fisica Nucleare
Dipartimento di Fisica – Università di Genova
Via Dodecaneso 33 – 16146 – Genova – Italy

ABSTRACT

The splitting between the charge-longitudinal and spin-transverse responses is explained in a model whose inputs are the effective interactions in the particle-hole channels in the first order boson loop expansion. The interplay between ω -meson exchange and box diagrams mainly governs the longitudinal response, while in the transverse one the direct Δ excitations almost cancel the one-loop correction and the response is ruled by the ρ -meson rescattering.

1 The experimental and theoretical situations

The experimental outcomes in the quasi-elastic peak (QEP) region are at present still controversial both on the experimental and theoretical point of view.

Starting from $\frac{d^2\sigma}{d\Omega d\epsilon} = \sigma_M \{v_L R_L(q, \omega) + v_T R_T(q, \omega)\}$ the Saclay experimentalists [1, 2] were able to perform the Rosenbluth separation thus getting both R_L and R_T . The longitudinal response was drastically quenched with respect to the Free Fermi Gas (FFG) model, while the transverse one was remarkably increased.

The first difficulties came from the non-fulfillment of the Coulomb sum rule, that, being expected to provide the nuclear charge, was quenched to a, say, 90% in case of ^{12}C but to a 60% in the case of ^{40}Ca .

Few years ago the Rosenbluth separation has also been performed at Bates [3]. The quenching of the sum rule for the ^{40}Ca turned out to be of about a 10%, in sharp contrast with the Saclay data.

Very recently Jourdan [4] outlined that the Rosenbluth separation is not free from theoretical ambiguities, and others are introduced in deriving the sum rule: the distortion of the outgoing electron must be correctly accounted for, before separating the channels; further, relativity prevents us to define the Coulomb sum rule in a natural way [5]. Jourdan showed that the corrected sum rule derived from world set of data is compatible with Z within a 1% uncertainty.

This outcome is, in principle, not strongly contradictory with the Saclay results: the Coulomb sum rule in fact properly reads $\int_0^\infty R_L(q, \omega)/G_E^2(q^2) \simeq S_L(q) = Z + \frac{2Z}{p}g(q)$, $g(q)$ being the pair correlation function, and the outcome of [4] only states that $g(q)$ is compatible with 0 at, say, $q = 570$ MeV/c. At lower momenta still a sizeable quenching survives.

Coming to the theory, all approaches agree in providing a more or less pronounced

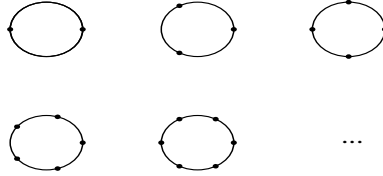


Figure 1: The bosonic effective action. Dots denote the external points.

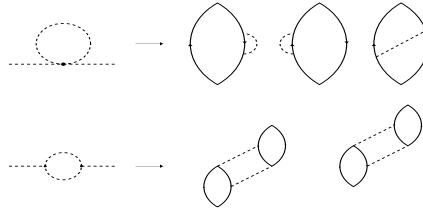


Figure 2: First order diagrams in the BLE. Recall that the dashed lines always describe RPA-dressed bosons

been less investigated. Ref. [9] seems to be (up to our knowledge) the only attempt to explain simultaneously the two response within the same frame, namely that of continuum RPA plus two-body currents. Still, both responses seem to be slightly overestimated.

2 The theoretical frame

Our starting point in [10] was to build up a well-behaved approximation scheme for a system of nucleons and pions. The idea of the bosonization arose quite naturally there, as it was obtained by representing the generating functional of the system by means of a Feynman path integral and by integrating over the fermionic degrees of freedom. Then the system turns out to be described by the bosonic effective action

$$S_B^{\text{eff}} = \frac{1}{2} \int d^4x d^4y \phi(x) [D_0]^{-1} (x - y) \phi(y) \quad (1)$$

$$- \sum_{n=2}^{\infty} \int d^4x_1 \dots d^4x_n \frac{1}{n} \Pi^{(n)}(x_1, \dots, x_n) \phi(x_1) \dots \phi(x_n),$$

ϕ denoting the pion field, D_0 its free propagator and the nonlocal vertices $\Pi^{(n)}(x_1, \dots, x_n)$, that keep memory of the fermion dynamics, being shown in fig. 1. This action generates a new class of approximations – or a recipe to collect classes of Feynman diagrams together – when the semiclassical expansion is carried out. This scheme is referred to as boson loop expansion (BLE).

The recipe to classify a Feynman diagram according to its order in BLE is to shrink

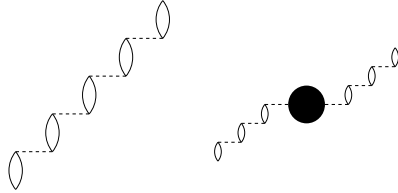


Figure 3: Diagrams pertaining to the response function at the one-loop level. The black bubble summarizes the 5 diagrams of fig.2 dashed lines always describe RPA-dressed bosons

Thus the mean field level coincides with the RPA, as can be seen diagrammatically. At the linear response level the mean field is thus described by the RPA-dressed polarization propagator if the probe has the same quantum numbers of the pion or, if not, by the bare Lindhard function. At the one-loop order the only possible diagrams are those of fig. 2. The full response at the one-loop order is given by the imaginary part of the diagrams of fig. 3, where the black bubble denotes the sum of all the diagrams of fig. 2.

It is evident from fig. 2 that only fermion loops with at most four external legs intervene at the one-boson-loop order. This fact is of overwhelming relevance since analytical expressions are available for them [11, 12] at least in the nonrelativistic kinematic.

The pion condensation is unavoidably met in the RPA scheme if we only allow pion exchange without accounting for short range correlations (SRC). To avoid it we are forced to forbid its occurrence by phenomenologically embedding SRC in our model by means of the Landau parameter g' , that here plays the role of a potential.

To adhere to phenomenology we are thus forced to change somehow our approach and to adopt a potential frame: D_0^{-1} is replaced by the inverse potential in the given p-h channel (meson exchange plus Landau parameter) and the field ϕ is reinterpreted as an auxiliary field. The topology of the diagrams remains unchanged.

In going from the mean field to the one loop level, a qualitative change is met. In the former case not too high momenta enter the dynamics, while in the latter the loop momentum is integrated over and the high momentum behaviour of the effective interaction rules the convergence of the integral. This is exploited by forcing a q -dependence in g' such that $g'(q) \xrightarrow{q \rightarrow \infty} 1$. But this in turn requires the introduction of a further cut-off related to the SRC range and which becomes the crucial parameter ruling the one loop corrections.

So far we have only discussed a system of nucleons and only one effective interaction. The dynamics required to describe the nuclear responses is by far richer. Other channels are accounted for by simply interpreting the dashed lines in figs. 2 as a sum over all the allowed channels. Also, the excitation of the nucleons to a Δ can be allowed by interpreting each solid line as a nucleon or as a Δ and again summing over all possible cases. *Remarkably the topology of the diagrams does never changes.*

3 The dynamical model

We shall consider here the (correlated) exchange of π , ρ and ω -mesons. In each particle-hole channel the interaction will read

$$V_m(q) = \frac{f_{\pi BB'}^2}{m_\pi^2} \left\{ g'_m(\mathbf{q}) - C_m \frac{\mathbf{q}^2}{m_m^2 + \mathbf{q}^2} \right\} v_m^2(q^2), \quad (2)$$

where the index m runs over the accounted channels and $B = N$ or Δ .

Concerning the pion, by definition, we have $C_\pi = 1$.

A vector meson interact with the nucleons via a Coulomb-like plus a spin-transverse interaction plus eventually an anomalous spin current. Customarily the convective current is neglected.

Since the ‘‘anomalous magnetic moment’’ is absent in the ω case, the coupling constants of the Coulomb-like and spin-transverse interactions would coincide, while the anomalous spin current of the ρ will dominate. We shall also account for the interaction of the ρ meson with the nuclear medium other than ph and Δ h excitations (we means for instance $\rho \rightarrow \pi\pi$ with further interaction of pions with the medium) by attributing to the ρ (in the spin-transverse channel only) an effective mass.

Remarkably the ρ -exchange, due to its high mass and its vector character, is essentially perturbative and the coupling constant can be invoked from the phenomenology, while coming to the ω meson, we have left the interaction in the spin-transverse channel unchanged, since it is weak, but the Coulomb-like interaction needs to be drastically renormalized in the medium.

The Landau parameter g' is present in the isovector spin-transverse and spin longitudinal channels only, where it has been parametrized according to

$$g'_{L,T}(q) = C_m + (g'_0 - C_m) \left[\frac{q_{cL,T}^2}{q_{cL,T}^2 + q^2} \right]^2 \quad (3)$$

in such a way that for $q \rightarrow 0$ $g'_{L,T}(q) \rightarrow g'_0$ and for $q \rightarrow \infty$ the right behaviour is achieved. The further cut-offs are called here $q_{cL,T}$.

4 The mean field level

The mean field level in a coherent discussion is expected to precede the first order corrections, and we shall follow this aptitude in the present exposition. The situation at hand however is particularly unlucky, because the mean field level is inextricably linked in the present case to the one-loop corrections. In fact:

1. In the charge-longitudinal channel the mean field is mainly dominated by the ω exchange, which is repulsive and so entails a quenching of the response. As a simple mathematics shows this implies also a hardening of the response [13] that is not observed in the data. Further, we neglected in our approach the σ -meson exchange, which is known from the Dirac phenomenology [14, 15, 16] to be attractive and that cancels to a large amount with the ω exchange. In our approach, in the same line of

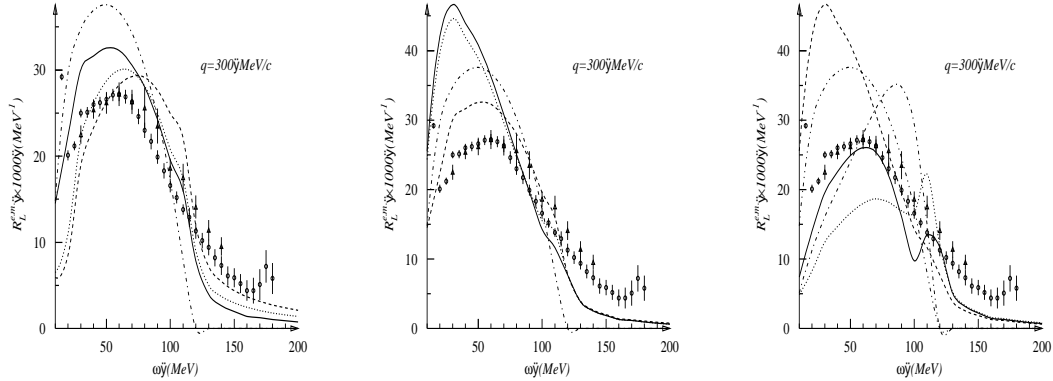


Figure 4: Left: the longitudinal response for ^{12}C without RPA dressing of the mean field and without Δ 's. Dash-dotted line: FFG; dashed line: FFG plus self-energy diagrams; dotted line: FFG plus self-energy and exchange diagrams; solid line: FFG plus self-energy, exchange and correlation diagrams.

Center: as before but with Δ 's. Dash-dotted line: FFG; dashed line: diagrams without Δ ; dotted line: box diagrams added diagrams; solid line: full calculation.

Right: the full response. Solid line: full response; dashed line: all diagrams without RPA; dotted line: diagrams without Δ 's only but with RPA; dash-dotted line: mean field; dash-dotted-dotted line: FFG

resonance. These diagrams are contained indeed in our correlation diagrams, which are however at the one-loop level.

2. In the transverse channel the one-loop corrections are strongly suppressed (we shall see later that the Δ -excitation makes this job). Thus the mean field becomes dominant in explaining the response and in turn it is ruled by the effective interaction in the ρ channel. Thus in view of our assumption (suppression of one-loop corrections) we can extract information about the effective interaction from the data.

5 The one-loop corrections

We finally come to the one-loop corrections.

First, let us define once forever the sets of parameters we shall use.

The mass of the ρ -meson has been set to 600 MeV in the spin-transverse channel. The pion coupling constant have been assumed, as usual, as $\frac{f_{\pi NN}^2}{4\pi} = 0.08$, $\frac{f_{\pi N\Delta}^2}{4\pi} = 0.32$ and $\frac{f_{\pi\Delta\Delta}^2}{4\pi} = 0.016$. Next, $C_{\rho NN} = C_{\rho N\Delta} = C_{\rho\Delta\Delta} = 2.3$ in the spin-transverse channel and $= 0.05$ in the scalar-isovector one. Further, $C_{\omega NN} = C_{\omega\Delta\Delta} = 0.15$ in the scalar-isoscalar channel and $= 1.5$ in the isoscalar spin-transverse one (all these results are in agreement with those of the Bonn potential, except $C_{\omega NN}$ in the scalar-isoscalar channel, that is essentially a free parameter). g'_0 is set to 0.35. The many-body cut-off of SRC are put

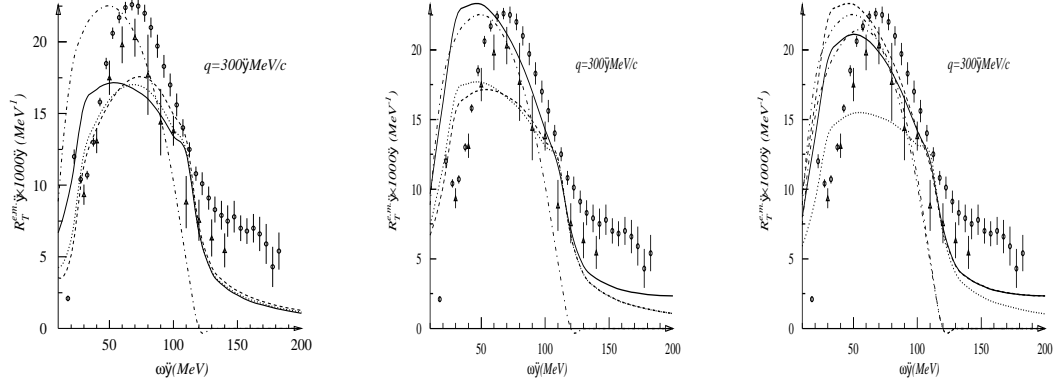


Figure 5: Left: the spin-transverse response for ^{12}C without RPA dressing of the mean field and without Δ 's. Dash-dotted line: FFG; dashed line: FFG plus self-energy diagrams; dotted line: FFG plus self-energy and exchange diagrams; solid line: FFG plus self-energy, exchange and correlation diagrams.

Center: as before but with Δ 's. Dash-dotted line: FFG; dashed line: diagrams without Δ ; dotted line: box diagrams added diagrams; solid line: full calculation.

Right: the full response. Solid line: full response; dashed line: all diagrams without RPA; dotted line: diagrams without Δ 's only but with RPA; dash-dotted line: mean field; dash-dotted-dotted line: FFG

the spin-transverse channel is $\Lambda_{\rho NN} = 1750 \text{ MeV}/c$ and finally all the remaining cut-offs at the vertices are set to $1000 \text{ MeV}/c$.

Let us start with the longitudinal response and examine, as a guideline, the case of Carbon at a transferred momentum of $300 \text{ MeV}/c$.

First let us examine the case of pure nucleon dynamics (no Δ 's) and also drop RPA dressing (this means that only the black bubble of fig. 3, corresponding to the five diagrams of fig. 2 survives). The main effects come from the isovector spin-longitudinal and spin-transverse channels, that turn out to be rather similar, while the other channels give a negligible contribution. In fig. 4(left) these one-loop corrections are shown, and, while going in the right direction, are still not sufficient to explain the quenching of the peak.

The next step is to introduce the Δ -resonance. On physical grounds we expect that box diagrams will dominate the response. They are shown in fig. 4(center) together with a complete calculation, i.e., with all possible diagrams. The box diagrams are dominant indeed and that they make the job the σ -meson is expected to do, namely to strongly enhance and (more important) to soften the peak. Finally in fig. 4(right) we plot the complete graph, with the inclusion of the RPA dressing everywhere. The net effect is clearly to cancel the enhancement induced by the box diagrams in such a way to come back to the experimental data, thus accomplishing the expected compensation between σ - and ω -meson as expected from Dirac phenomenology.

Next we examine the transverse response, following the same path as before. In fig.

without Δ 's. The path is clearly similar to that fig. 4 and is even more pronounced, but in the wrong direction, however.

The contribution of the Δ diagrams is then shown in fig. 5(center), again without RPA-dressing. This time an important difference arises, concerning the contribution of the box diagrams, that are almost irrelevant. Finally in fig. 5(right) the whole calculation is reported.

Here the physical insight are clear: since one-loop corrections are negligible, we are now sensitive to the RPA-dressing of the ρ -meson channel (the dominant one): we require here an effective interaction near to vanish, in order not to further deplete the peak. The one we have chosen is still a little bit repulsive: clearly the momentum region between 300 and 400 MeV/c is the most sensitive to the details of the effective interaction. As a matter of fact our results stay more or less between Saclay's and Jourdan's data.

A more complete survey of our results for ^{12}C is presented in fig. 6.

The figures 7 present instead the results of our calculation on ^{40}Ca . In this case we have assumed an higher value for k_F , namely $k_F=1.2 \text{ fm}^{-1}$, which better describes a medium nucleus. The interplay between RPA dressing of the external legs of the diagrams and the one-boson-loop corrections, which also alter the real part of the diagram (a density-dependent effect) leads to a more pronounced depletion of the longitudinal response, in agreement with the Saclay data. This results is relevant in our opinion and deserves a comment. For a long time the apparent discrepancy between the Saclay data on Carbon and Calcium, that provide so different Coulomb sum rule, led some people to question about the Calcium data. We have shown here that such a discrepancy may be explained as a density effect in the frame of a well defined theoretical model (the boson loop expansion) without violating the Coulomb sum rule.

Finally, we want to discuss the discrepancies between Saclay and Jourdan data. These are particularly emphasized in the transverse response. Recalling our previous discussion, the Jourdan data seem to require a less pronounced attraction in the isovector spin-transverse effective interaction. Since we decreased in our calculations the ρ -mass just to emphasize the attractive part of the interaction it is sufficient to keep for the ρ -mass its value in the vacuum to better agree with the Jourdan data. Considering however that still the uncertainty in the experimental situation survives and that no microscopical calculations are presently available for the ρ -meson mass in the nuclear medium, further discussions on this topic are still premature.

References

- [1] Z. E. Meziani et al. *Phys. Rev. Lett.*, 52:2180, 1984.
- [2] Z. E. Meziani et al. *Phys. Rev. Lett.*, 54:1233, 1985.
- [3] T. C. Yates et. al. *Phys. Lett.*, 312B:382, 1993.
- [4] J. Jourdan. *Phys. Lett.*, B353:189, 1995.
- [5] M. B. Barbaro et al. *Nucl. Phys.*, B569:701, 1994.

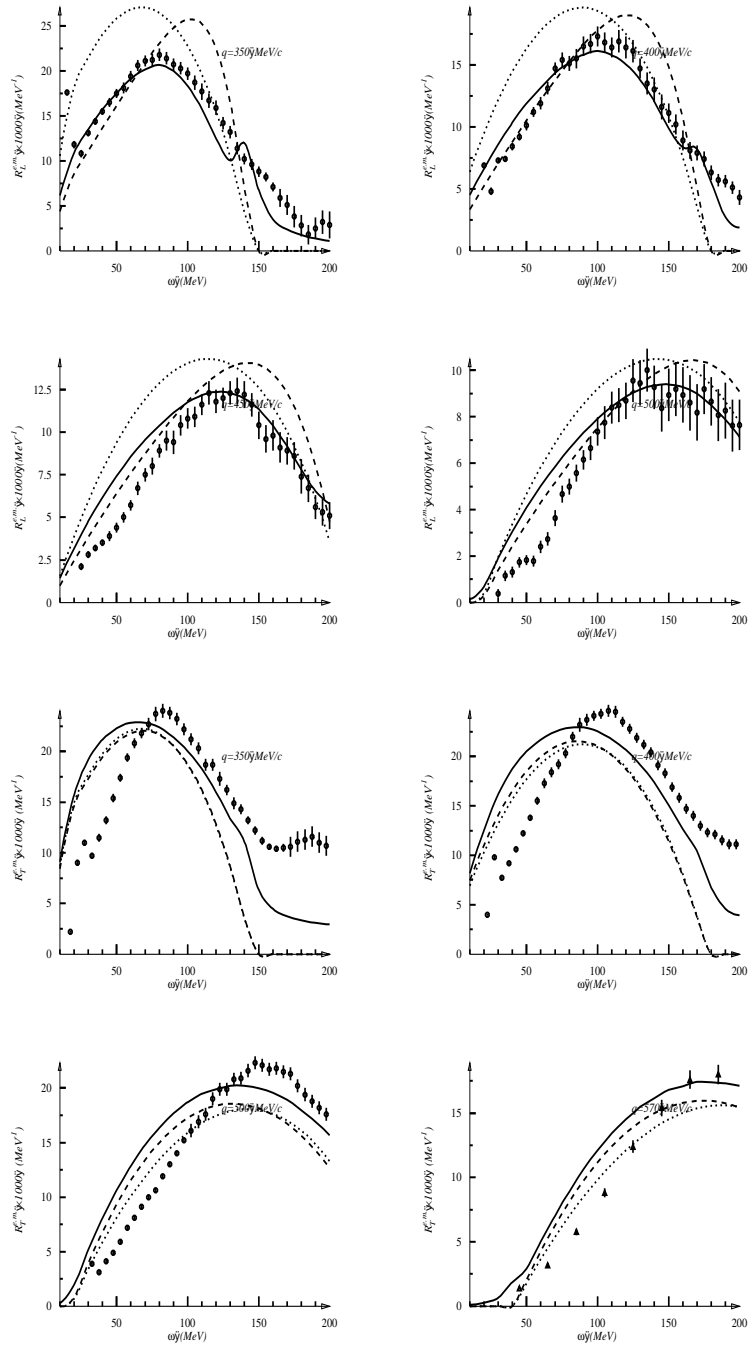


Figure 6: Full calculation for the longitudinal (two upper lines) and transverse (two lower lines) responses on ^{12}C at different transferred momenta. Data from [1, 2] (circles) and from [4, 19] (triangles). Solid line: full calculation dashed line: Mean field calculation dotted line: FFG calculation.

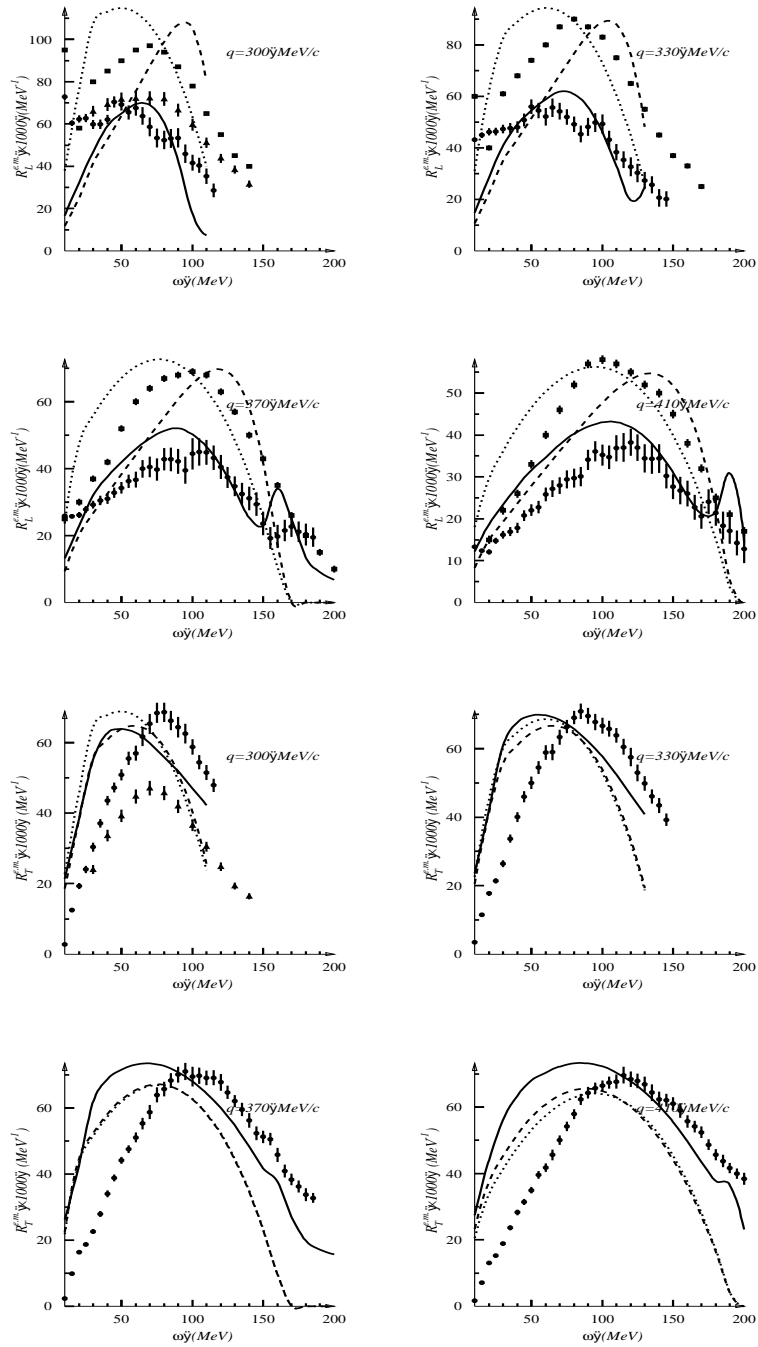


Figure 7: Full calculation for the longitudinal (two upper lines) and transverse (two lower lines) responses on ^{40}Ca at different transferred momenta. Data from [1, 2] (circles) and from [4, 19] (triangles). Solid line: full calculation dashed line: Mean field calculation dotted line: FFG calculation.

Figure 8: Full calculation for the transverse response on ^{40}Ca at different transferred momenta. Data from [1, 2] (circles) and from [4, 19] (triangles). Solid line: full calculation dashed line: Mean field calculation dotted line: FFG calculation.

- [7] G. P. Cò, K. F. Quader, R. D. Smith and J. Wambach. *Nucl. Phys.*, A485:61, 1988.
- [8] M. Barbaro et al. To be published on *Nucl. Phys. A*.
- [9] V. Van der Sluys, J. Rickebusch and M. Waroquier. To be published on *Phys. Rev. C*.
- [10] W. M. Alberico, R. Cenni, A. Molinari and P. Saracco. *Ann. of Phys.*, 174:131, 1987.
- [11] R. Cenni and P. Saracco. *Nucl. Phys.*, A487:279, 1988.
- [12] R. Cenni, F. Conte, A. Cornacchia and P. Saracco. *La Rivista del Nuovo Cimento*, 15 n. 12, 1992.
- [13] W. M. Alberico, R. Cenni, and A. Molinari. *Prog. in Part. and Nucl. Phys.*, 23:171, 1989.
- [14] J. D. Walecka. *Ann. Phys.*, 83:491, 1974.
- [15] B. C. Clark, S. Hama and R. L. Mercer. In H. O. Meyer, editor, *The Interaction Between Medium Energy Nucleons in Nuclei*, page 260. AIP Conference Proceedings, 1982.
- [16] B. C. Clark. In M. B. Johnson and A. Picklesimer, editor, *Relativistic Dynamics and Quark-Nuclear Physics*, page 302, New York, 1986. J. Wiley & Sons.
- [17] R. Machleidt, K. Holinde and Ch. Elster. *Phys. Rep.*, C149:1, 1987.
- [18] K. Holinde. *Phys. Rep.*, C68:121, 1981.
- [19] J. Jourdan. *Nucl. Phys.*, A603:117, 1996.